

# Fatigue-Crack-Growth Behavior of Ultrafine-Grained Al-Mg-Sc alloy Produced by ECAP

E. Avtokratova<sup>1a</sup>, O. Sitdikov<sup>1,2b</sup>, R. Kaibyshev<sup>3c</sup>, Y. Watanabe<sup>2d</sup>

<sup>1</sup>Institute for Metals Superplasticity Problems, Khalturina 39, Ufa 450001, Russia

<sup>2</sup>Nagoya Institute of Technology, Nagoya 466-8555, Japan

<sup>3</sup>Belgorod State University, Belgorod 308034, Russia

<sup>a</sup> lena@imsp.da.ru, <sup>b</sup> sitdikov.oleg@nitech.ac.jp, <sup>c</sup> rustam\_kaibyshev@bsu.edu.ru, <sup>d</sup> yoshimi@nitech.ac.jp

**Keywords:** fatigue, crack growth rate, aluminum alloy, warm-to-hot ECAP, UFG structure.

**Abstract.** Fatigue-crack-growth in an ultrafine-grained (UFG) Al-6%Mg-0.3%Sc alloy is investigated in conjunction with a precise analysis of the fracture surface. The comparison of the crack growth behavior of the UFG and ordinary polycrystalline materials has shown that the fatigue crack growth rate in the UFG alloy is higher than that in the coarse-grained material only in the near-threshold region. In the intermediate fatigue stage, propagation of the fatigue-crack in the UFG structure becomes insensitive to the grain size. At larger stress-intensity-factor-increments,  $\Delta K$ , the crack resistance of the UFG material is better than that of un-ECAPed specimen. Analysis of the surface features indicates that such inhibition of the crack growth in the UFG structure upon increasing  $\Delta K$  may be related to the gradual transition from intergranular- to transgranular mode of fatigue fracture.

## Introduction

In recent years there has been an increasing interest in the production of ultrafine-grained (UFG) materials by means of intense plastic straining (IPS) for both commercial and investigative purposes [1]. These materials exhibit mechanical and physical properties, which are out of the ordinary and of great interest, in particular their remarkable strength and toughness and their potential for superplasticity at low temperatures [e.g. 1-3]. A respectable amount of works [4-7] has also been focused to date on the effect of UFG structures on *fatigue properties*, as well as on the fundamental aspects of the behavior of UFG materials under cyclic loading conditions.

Traditionally, the total fatigue life of a metallic material is divided into two stages, namely, the stage prior to crack initiation and the stage of crack propagation. It has been well established now that the grain refining down to submicrocrystalline region after IPS may normally extend the crack initiation stage due to the improvement of the strength of material [8]. On the other hand, the fatigue crack growth behavior still remains least studied among other mechanical properties of UFG materials. It has been shown [4,6,7] that the resistance of UFG polycrystals to fatigue crack growth may be lower in the near-threshold region of the crack propagation than that of coarse-grained ones, as the fatigue fracture in the UFG structure occurs more readily in the *intergranular* manner and can be attributed to a less tortuous crack path. At the same time, a more ductile *transgranular* mode of the crack distribution with striations, corresponding to crack tip retardation and blunting, has been reported for some UFG Al- and Cu-alloys both under low- and moderate-to-larger stress-intensity-factor-increments conditions [9]. Unfortunately, the morphological features of the fatigue fracture appeared in a wide interval of the loading parameters are still poorly examined. As a result, the precise mechanisms of cyclic degradation in submicrocrystalline grain structures are undisclosed yet due to the lack of the related experimental data. The objective of this study is, therefore, to investigate the fatigue-crack-growth behavior of an Al-6%Mg-0.3%Sc alloy with an UFG structure introduced by IPS. This alloy is an advanced structural material for automotive and aviation industry and, hence, the evaluation of the potentiality of improvement of its fatigue properties by means of IPS seems to be very important for commercial application. Upon the measurement of the fatigue-crack-growth rate, specific attention in the current work is paid to analyze the

morphological features of the fracture surface along the crack path to elucidate the main mechanisms of the fatigue-crack propagation.

### Experimental

The alloy used had the following chemical composition (in mass %): 6Mg, 0.3Sc, 0.4Mn, 0.2Si, 0.1Fe and the balance Al. The as-extruded rod was fabricated at the Kamensk-Uralsk Metallurgical Works (Russia) by casting and hot extrusion that was performed at 390°C to a strain of about 0.7, followed by annealing at 400°C for 1h. After extrusion and annealing, the alloy was composed of a non-uniform partially recrystallized microstructure with a bimodal distribution of the grain size, namely, coarse elongated grains lying parallel to the extrusion axis, and fine equiaxed grains in their mantle regions (Fig. 1(a)). The size of coarse grains was around 170 and 70  $\mu\text{m}$  in longitudinal and transverse directions, respectively. The fine grains had the average size of 4.4  $\mu\text{m}$  and the volume fraction of 0.35<sup>1</sup>. Samples for ECAP were machined parallel to the extrusion axis into square plates having dimensions of 152×152×25 mm<sup>3</sup>. ECAP was carried out at 325°C using a die with a rectangular cross-section of 152x25 mm<sup>2</sup> and channel inner and outer angles of  $\Phi=90^\circ$  and  $\psi=0^\circ$ . These angles led to a strain of about 1 in each ECAP passage. The samples were pressed to 8 passes through route Bcz, i.e. the plate was rotated by 90° in the same sense around the normal axis to the plate between each pass [11]. After ECAP, the alloy had an almost uniform UFG structure with the grain size of about 1  $\mu\text{m}$  and the volume fraction of about 0.88 (Fig. 1(b)). Besides, some remnant parts of original grains were present in this structure.

Compact tension (CT) specimens used in fatigue crack propagation tests had thickness of 20 mm. The specimens were cut from ECAP plate, so that the crack growth direction was parallel to the last ECAP axis. Axial fatigue tests were conducted with the load ratio  $R=0.1$  and initial stress intensity factor range  $\Delta K = 5.5 \text{ MPa} \cdot \text{m}^{0.5}$  using a hydraulic testing machine “Shenk hydropuls PSA” operating at a sinusoidal frequency of 5Hz in laboratory air at ambient temperature. The stress intensity factor,  $K$ , and the crack growth rate,  $da/dN$ , were calculated according to the equations provided by ASTM Standard E647. The crack surface profile of fatigue tested specimens was analyzed using a “Nikon L-150” optical microscope. The fracture surfaces were examined at various distances from the original crack tip by a scanning electron microscope “JEOL JXA -6400”.

### Results and Discussion

**Fatigue crack growth rate.** Fig. 2 represents the dependence of the fatigue-crack-growth rate,  $da/dN$ , in UFG Al- 6%Mg-0.3%Sc alloy (filled symbols) and original coarse-grained alloy (see Fig. 1, open symbols) on the stress intensity factor range,  $\Delta K$ .

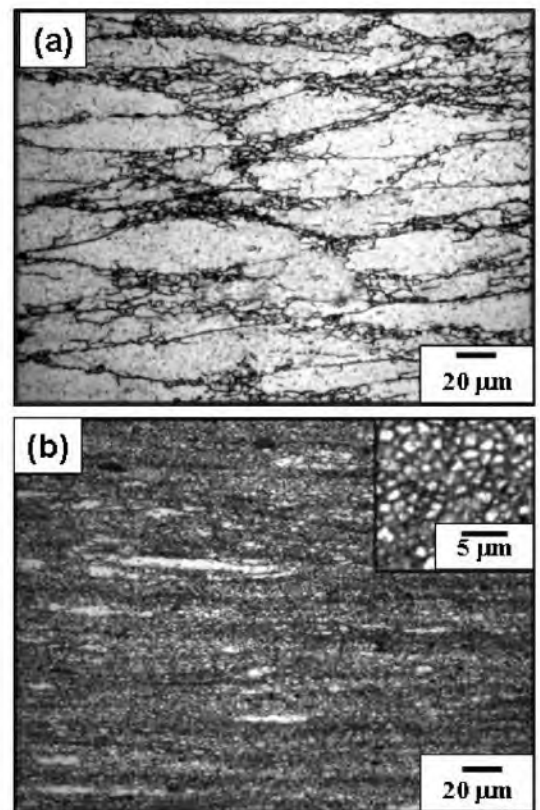


Fig. 1 Typical microstructures of Al-6%Mg-0.3%Sc alloy: (a) before ECAP; (b) after 8 ECAP passes,  $T=325^\circ\text{C}$ , route Bcz; the last pressing direction is horizontal.

<sup>1</sup> More details for the original structure of the present alloy are described elsewhere [10].

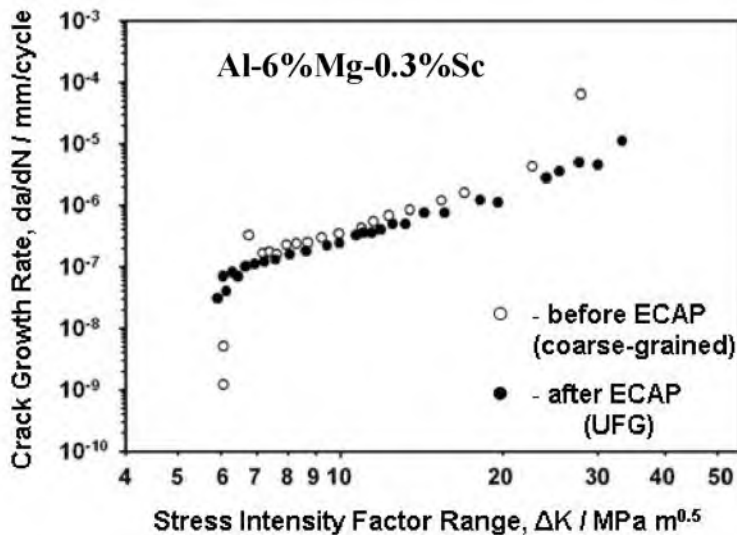


Fig. 2 Fatigue crack growth rate in UFG Al-6%Mg-0.3%Sc alloy produced by ECAP. Data for coarse-grained Al-6%Mg-0.3%Sc alloy are plotted for comparison.

It can be seen that the dependence plotted for the ordinary polycrystalline material exhibits the three well-known stages of crack propagation, i.e. (i) a stage of slow crack advance in the near threshold region ( $\Delta K \leq 6.5 \text{ MPa} \cdot \text{m}^{0.5}$ ); (ii) an intermediate (the Paris regime,  $da/dn \sim (\Delta K)^m$  [12]) stage ( $6.5 < \Delta K < 20 \text{ MPa} \cdot \text{m}^{0.5}$ ); and (iii) a stage of unstable crack growth at high  $\Delta K$  values ( $\Delta K > 20 \text{ MPa} \cdot \text{m}^{0.5}$ ). Also, it is seen in Fig. 2 that in the UFG state, the stage (ii) of fatigue crack propagation is remarkably extended toward the higher  $\Delta K$  region, whereas the stage (iii) becomes less prominent. The crack growth rate in this material in the near threshold region (i) is higher than that in the ordinary polycrystalline state; however, on the intermediate fatigue

stage (ii), the rates of crack propagation in both materials approach to the roughly same values of  $da/dN$ . This suggests that while in the near-threshold region, the fatigue crack growth behavior is influenced by the microstructural factors, the crack growth in the present UFG material at relatively large  $\Delta K$  may occur to be insensitive to the grain size. Note that similar fatigue-crack-growth behavior, when the microstructure has less influence on the crack propagation in the Paris regime, has been reported for some UFG materials in some works [e.g. 4,6,9]. Previously, such effect was also observed on the conventional coarse- / fine- grained materials [e.g. 13,14] and thus, this may be a common phenomenon for the polycrystals lying in a wide range of grain sizes. However, only limited information is still available on the detailed influence of UFG microstructure on fatigue crack growth behavior, especially in the large- $\Delta K$  regime. As it can be seen in Fig. 2, the resistance of the UFG structure to the fatigue-crack-grow may be somewhat increased by the transition to the moderate-to-high  $\Delta K$  range ( $\Delta K \geq 20 \text{ MPa} \cdot \text{m}^{0.5}$ ). As a result, the final fracture of the coarse-grained samples takes place at  $\Delta K \sim 27 \text{ MPa} \cdot \text{m}^{0.5}$ , while the UFG samples are fractured at  $\Delta K \sim 33 \text{ MPa} \cdot \text{m}^{0.5}$ . Such effect of  $\Delta K$  on the rate of the crack propagation seems to be related with a change in the mechanisms of the fatigue fracture. Let us provide the detailed analysis of the specific features of crack distribution in the UFG samples in the whole low-to-moderate/moderate-to-high  $\Delta K$  region in conjunction with the data represented in Fig. 2.

**Fatigue crack path in the UFG material.** The typical pictures that show the profile of the fatigue crack in the UFG material (a) at transition from the near threshold region to the intermediate stage of the crack propagation, i.e. at  $\Delta K \sim 7 \text{ MPa} \cdot \text{m}^{0.5}$ ; (b) at the middle part of the intermediate stage, i.e. at  $\Delta K \sim 9 \text{ MPa} \cdot \text{m}^{0.5}$  and (c) at the end of the intermediate stage, i.e. at  $\Delta K \sim 18 \text{ MPa} \cdot \text{m}^{0.5}$ , are represented in Fig. 3. It is seen in Fig. 3(a) that the propagation of the crack in the near threshold region and at the beginning of the intermediate stage is characterized by a relatively small roughness of the fracture surface. However, the crack path becomes more tortuous by crack growth in the intermediate stage (Figs. 3 (b) and (c)). At that the crack propagation starts to occur in a zigzag manner. Note that from a macroscopic point of view, such crack path serration causes an increase in the total length of the crack path. This increment testifies to a larger area of fracture surfaces and, consequently, to larger work needed for crack growth at higher  $\Delta K$ .



Fig. 3 Fatigue crack surface profile in UFG Al-6%Mg-0.3%Sc alloy developed at various distances,  $\Delta L$ , from the initial crack tip: (a)  $\Delta L = 4$  mm ( $\Delta K \sim 7$  MPa  $m^{0.5}$ ); (b)  $\Delta L = 7$  mm ( $\Delta K \sim 9$  MPa  $m^{0.5}$ ); (c)  $\Delta L = 13$  mm ( $\Delta K \sim 18$  MPa  $m^{0.5}$ ).

**Fracture surface features.** Fig. 4 shows the typical fragments of the fracture surface, which correspond to (a) the near-threshold region; (b) and (c) the intermediate stage of the fatigue crack growth and (d) the beginning of the unstable crack growth stage. It is seen in Fig. 4 (a) that in the near-threshold region, i.e. at low values of  $\Delta K$ , the fracture mode of the UFG sample is mostly faceted and brittle-like. The size of the fracture facets ( $\sim 1$ - $2$   $\mu m$ ) that are formed in this stage roughly coincides with the grain size introduced by ECAP (see Fig. 1(b)). This suggests that at the low-to-moderate  $\Delta K$  values, the fatigue crack growth in the present material occurs in the preferred intergranular manner.

In the intermediate fatigue stage, i.e. in the higher  $\Delta K$  region, a progressive coarsening of the fracture surface takes place (Figs. 4 (b) and (c)). The size of facets is gradually increased with

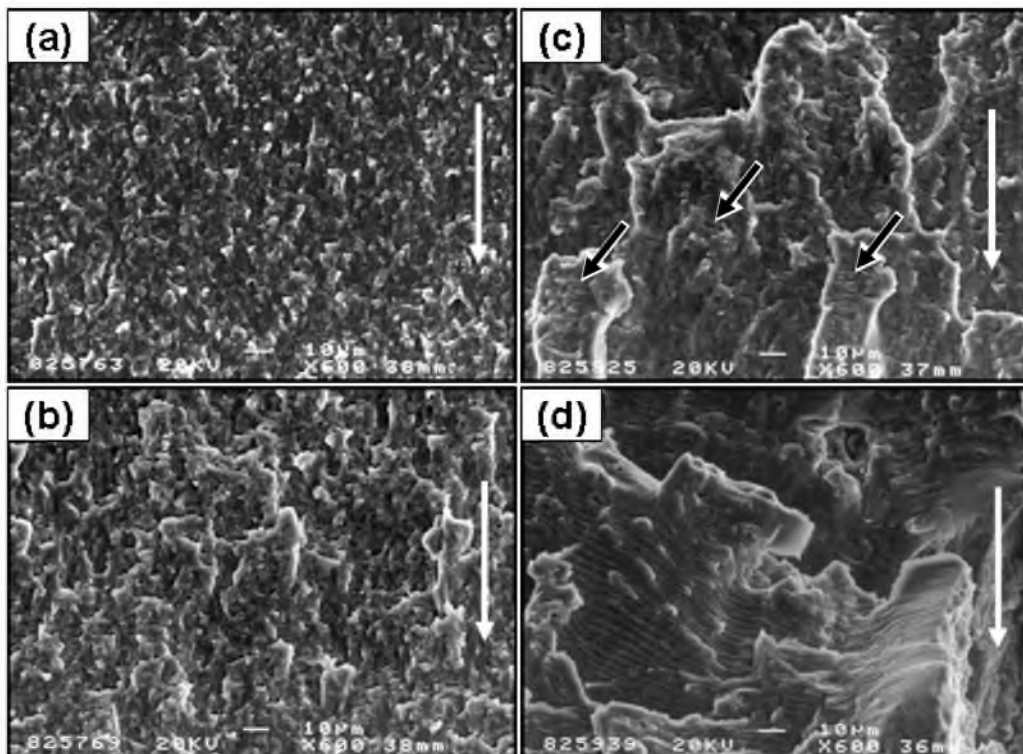


Fig. 4 Typical micrographs of fatigue fracture surface features appeared in UFG Al-6%Mg-0.3%Sc alloy at: (a)  $\Delta K \sim 6.5$  MPa  $m^{0.5}$  (low  $\Delta K$  region); (b)  $\Delta K \sim 9$  MPa  $m^{0.5}$  (low-to-intermediate  $\Delta K$  region); (c)  $\Delta K \sim 18$  MPa  $m^{0.5}$  (intermediate  $\Delta K$  region); (d)  $\Delta K \sim 25$  MPa  $m^{0.5}$  (high  $\Delta K$  region). White vertical arrows indicate the crack growth direction. Black arrows in (c) indicate weak striations.

increasing  $\Delta K$ , so that every facet “covers” a number of UFG grains. Thus, Fig. 4 ((a)-(c)) shows that the fatigue crack propagation becomes insensitive to the boundaries of individual UFG grains

by a transition to the stage (ii). This observation confirms the “structural insensitive” character of crack growth in the UFG structure mentioned in Fig. 2. Note that such “structural insensitivity” may be related to the gradual extension of the crack tip plastic deformation zone upon increasing  $\Delta K$  [9]. It can be assumed that the plastic zone dimension is commensurable with the micrometer grain size at the beginning of the crack propagation stage, while it becomes much larger than that at higher  $\Delta K$ . A large plastic zone can interact with several grains, thereby allowing the formation of common planar fracture surfaces in them. This may be obviously accompanied by a deflection of the crack path from the straight line (see Fig. 3).

Also it is seen in Fig. 4 that the mechanism of the fatigue fracture in the present UFG material is gradually changed from the intergranular fracture one, which takes place in the near threshold region, to transgranular one that occurs in the region of large  $\Delta K$ . At that some weak striations start to be revealed on the fracture surface at moderate-to-high  $\Delta K$  (as arrowed in Fig. 4(c)) indicating that the fatigue crack growth seems to occur by classical crack-tip blunting mechanisms that give rise to striation formation. Such striations accompanied by opening secondary cracks become more prominent upon the further increasing  $\Delta K$  toward the end of the intermediate- / beginning of the instable crack growth region (see Fig. 4 (d)). At the same time, there are no evidences of faceted and/or dimpled fracture in this stage. This suggests that the transgranular fracture mechanism is dominant in the large  $\Delta K$  range.

Thus, the present data clearly show that the intergranular fracture of the UFG samples at low values of the stress-intensity-factor-increments (Fig. 4(a)), which is accompanied by a low roughness of the fatigue crack path (Fig. 3(a)), provides worse crack resistance than the coarse-grained material (see Fig. 2). Note that the similar results were earlier obtained in [4,6,7]. At the same time, inhibition of the fatigue crack growth in the UFG material at relatively large  $\Delta K$  is related with the coarsening of the fracture surface, which is caused by a gradual transition from intergranular to transgranular mode of fatigue fracture upon increasing  $\Delta K$ .

**Effect of second phases on crack propagation.** The other important factor that can significantly affect the crack resistance of the present material is the presence of the second phase particles in the material structure [15]. Fig. 5 represents the typical optical micrographs of the polished surface of the present Al-Mg-Sc alloy (a) before- and (b) after ECAP. It can be seen that in the initial state, i.e. after the conventional thermomechanical treatment (see section *Experimental*), the alloy contains relatively coarse primarily particles (Fig. 5 (a)). The latter are classified in [16] as the intermetallics  $Al_6(Fe,Mn)$ . It is seen in Fig. 5(a) that these particles are distributed non-uniformly in the original structure and their size is varied from 5 to 30  $\mu m$ . During the cyclic

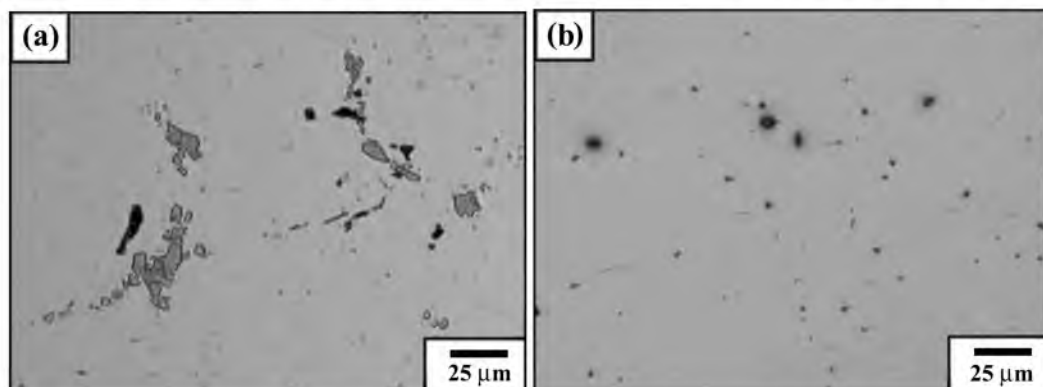


Fig. 5 Polished surface of the Al-6%Mg-0.3%Sc alloy: (a) before ECAP; (b) after 8 ECAP passes.

loading these can cause the stress concentration followed by a rapid nucleation of secondary cracks in the Al matrix [15]; the latter may grow and merge with the main crack, thereby reducing crack resistance. After ECAP (Fig. 5(b)), in contrast, the size of the second phases was found to be decreased to the submicrocrystalline scale range (see also microstructures represented in [10]) and

their distribution becomes more uniform, i.e. these phases are profoundly fragmented and/or dissolved during warm-to-hot IPS [17,18]. As the result, the harmful effect of the second phases on the rate of fatigue crack propagation becomes much weaker. In the other words, ECAP can provide additional improvement of the crack resistance in the present Al-Mg-Sc alloy due to a fragmentation and/or dissolution of coarse primarily particles during IPS.

## Summary

The fatigue-crack-growth behavior of an UFG (grain size  $\sim 1 \mu\text{m}$ ) Al-6%Mg-0.3%Sc alloy produced by warm-to-hot ECAP is investigated in the present work. The main results are summarized as follows.

1. In the near-threshold region, the UFG material exhibits a higher fatigue crack growth rate than in the original coarse-grained state. The low crack resistance in the UFG material in this stage is related to the preferred intergranular mode of fatigue fracture and low tortuous crack path.
2. In the intermediate fatigue stage, the crack propagation in the UFG structure becomes insensitive to the boundaries of UFG grains. At that, the crack growth is accompanied by a gradual change from intergranular fatigue fracture to transgranular one.
3. Change in the fracture mechanism mentioned in (2) is accompanied by a remarkable coarsening of the fracture surface and/or increasing the tortuosity of the crack path. This, hence, inhibits the crack propagation rate in the UFG material. As a result, at relatively large stress-intensity-factor-increments, the UFG material exhibits better fatigue crack growth resistance than original coarse-grained one.

This work was partially supported by “Grant-in-Aid for Scientific Research on Priority Areas (19025005)” by the Ministry of Education, Culture, Sports, Science and Technology of Japan.

## References

- [1] R.Z. Valiev, R.K. Islamgaliev, I.V. Alexandrov: *Progr. Mater. Sci.* Vol. 45 (2000), p. 103
- [2] S. Lee, P. Berbon, M. Furukawa, Z. Horita, et al.: *Mater. Sci. Eng.* Vol. A272 (1999), p. 63
- [3] N. Tsuji, Y. Saito, Y. Minamino: *Scripta Mater.* Vol. 47 (2002), p. 893
- [4] A. Vinogradov, S. Nagasaki, V. Patlan, K. Kitagawa and M. Kawazoe: *Nanostruct. Mater.* Vol. 11 (1999), p. 925
- [5] T. Hanlon, Y.-N. Known, S. Suresh: *Scripta Mater.* Vol. 49 (2003), p. 675
- [6] H.-K. Kim, M.-I. Choi, Ch.-S. Chung, D. H. Shin: *Mater. Sci. Eng.* Vol. A340 (2003), p. 243
- [7] P.S. Pao, H.N. Jones, S.F. Cheng, C.R. Feng: *Int. J. Fatigue* Vol. 27 (2005), p. 1164
- [8] M.K. Rabinovich, M.V. Markushev: *J. Mat. Sci.* Vol. 31 (1996), p. 4997
- [9] A. Vinogradov: *J. Mater. Sci.* Vol. 42(5) (2007), p. 1797
- [10] O. Sitdikov, T. Sakai, E. Avtokratova, R. Kaibyshev, Y. Kimura and K. Tsuzaki: *Mater. Sci. Eng.* Vol. A44 (2007), p. 18
- [11] M. Kamachi, M. Furukawa, Z. Horita, T. G. Langdon: *Mater. Sci. Eng.* Vol. A361 (2003), p. 258
- [12] P. Paris and F. Erdogan: *Trans ASME, J. Basic Eng.* Vol. 85 (1963), p. 528
- [13] R. Gürbüz and F. Sarioğlu: *Mater. Sci. Technol.* Vol. 17 (2001), p. 1539
- [14] D.A. Lados, D. Apelian: *Mater. Sci. Eng.* Vol. A385 (2004), p. 200
- [15] V. Yelagin: *Metal Sci. and Heat Treat.* No 9 (2002), p. 10
- [16] E. Avtokratova, O. Sitdikov: *Proc. of the Russian Conf. for Students and Young Scientists “Basic Research in Mathematics and its Application in Natural Science. Physics”* Ufa (2007), p. 18
- [17] Z. Zhang, S. Hosoda, I-S. Kima, Y. Watanabe: *Mater. Sci. Eng.* Vol. A425 (2006), p. 55
- [18] K.-T. Park, E.G. Lee, W.J. Nam, Y.S. Lee: *Mater. Sci. Forum* Vols. 539-543 (2007), p. 2859